THEF-NIJM 90.02

# Magnetic moment interaction in nucleon-nucleon phase-shift analyses*

V.G.J. Stoks and J.J. de Swart
*Institute for Theoretical Physics, University of Nijmegen, Nijmegen, The Netherlands*

## Abstract

The details of our procedure for including the magnetic moment interaction in nucleon-nucleon phase-shift analyses are given. The magnetic moment scattering amplitude in case of *pp* scattering is calculated in Coulomb distorted-wave Born approximation. Special attention is given to the construction of the nuclear amplitude in the presence of the complete electromagnetic (modified Coulomb, magnetic moment, and vacuum polarization) interaction. We compare our treatment with approximations that have appeared in the literature and show that these approximations are no longer found to be adequate for a proper description of recently published accurate scattering data.

PACS numbers: 21.30.+y, 13.75.Cs, 11.80.Et, 12.40.Qq



*Published in Phys. Rev. C **42**, 1235–1248 (1990).

## I. INTRODUCTION

The effects on nucleon-nucleon scattering arising on account of the interaction of the magnetic moment of a nucleon with the electromagnetic field of the partner nucleon have been known for a long time. The influence of the magnetic moment Coulomb interaction was first brought to general attention when Mott [1] pointed out the effects it has on the polarization resulting from electron scattering by nuclei. The importance of the interaction in neutron-nuclei scattering was discussed by Schwinger [2], who calculated in Born approximation its influence on the neutron polarization. His results indicated a pronounced effect for small-angle scattering.

The effects of including the magnetic moment (MM) interaction in the proton-proton scattering formalism have been discussed some decades ago by Breit [3], and Ebel and Hull [4], Breit and Ruppel [5], and Garren [6]. They calculated the MM scattering amplitude in plane-wave Born approximation, including some adjustments for Coulomb distortion effects. It was found that inclusion of this MM amplitude in their phase-shift analysis of at that time called high-energy ($T_{\rm lab} \gtrsim 150$ MeV) *pp* scattering data, resulted in a noticeable improvement in the description of the forward-angle analyzing power. This can be understood in view of the fact that the MM interaction gives rise to a long-range spin-orbit force, and so if the interaction is to be of any importance, this will first show up in a better description of the analyzing power $A_y$, which strongly depends on the spin-orbit interaction. In the low-energy region ($T_{\rm lab} \lesssim 50$ MeV), almost no analyzing power data existed, and the statistical errors on the data that were available are much larger than the effects that are expected from including the MM interaction. So it was argued that the MM effects could be neglected altogether in a low-energy *pp* phase-shift analysis.

In the mid-1970s this situation changed as new accurate *pp* $A_y$ data at $T_{\rm lab} = 10.0$ MeV became available [7], which warranted a reconsideration of the importance of the effects of the MM interaction. The forward-angle analyzing power at this energy displays a diplike structure. Inclusion of the plane-wave Born approximated MM scattering amplitude gives rise to an even more pronounced dip structure for the small-angle analyzing power, which is in disagreement with these 10-MeV data. This discrepancy was investigated by Knutson and Chiang [8]. They showed that the MM scattering amplitude should be calculated in Coulomb distorted-wave Born approximation (CDWBA) rather than in plane-wave Born approximation (BA). Inclusion of the Coulomb distortion has little effect on the magnitude of the MM amplitude, but it does change its phase. Because of this change in phase, the MM amplitude and the Coulomb amplitude are almost exactly in phase, and the increase in the forward-angle dip structure in the analyzing power is no longer present. This is in excellent agreement with the experimental data, which is dramatically shown in Fig. 1 of that paper [8]. As a result, the proper inclusion of the MM interaction has almost no influence on the description of the low-energy *pp* analyzing power. The experimental data appear to be described just as well when the effects of the MM interaction are entirely neglected. Therefore, it has still been customary to neglect these effects in the phase-shift analyses of the low-energy ($T_{\rm lab} \lesssim 30$ MeV) *pp* scattering data [9,10], whereas in the higher-energy *pp* phase-shift analyses [11–15] these effects are (approximately) taken into account.

Recently, a very accurate *pp* $A_y$ experiment at 50.04 MeV has been finished [16]. Because of the very high accuracy of this experiment, the proper inclusion of the MM interaction in a $pp$ phase-shift analysis has become important. Approximations for including the effects of the MM interaction which have appeared in the literature are now no longer found to be acceptable. This has been shown explicitly by us in a recent paper [17], where we analyze these 50-MeV $A_y$ data.

The influence of the MM interaction in neutron-proton scattering was investigated by Hogan and Seyler [18] in a nonrelativistic framework. Inclusion of the MM amplitude gives rise to a pronounced dip structure in the $np$ analyzing power. Contrary to the $pp$ analyzing power, this dip structure in the $np$ analyzing power is not present in the absence of the MM amplitude. In their calculations over an energy-range of 25–210 MeV, Hogan and Seyler found that the influence of the MM interaction on the description of the $np$ scattering observables is indeed significant, but only for small ($< 5°$) center-of-mass scattering angles. At lower energies the influence is probably extended to larger angles. However, the accuracy of the $np$ scattering data has always been rather poor compared with the accuracy of the $pp$ scattering data. The effects of the MM interaction are almost always smaller than the statistical errors on these data, which makes these effects of negligible importance. Nevertheless, the $np$ MM scattering amplitude can be incorporated without any difficulty, and it has been included in the more recent $np$ phase-shift analyses [11,12,19].

About a year and a half ago, new accurate $np$ $A_y$ measurements have become available at 10.03 MeV [20] and 16.9 MeV [21]. Measurements at even lower energies are in progress [22]. These data include forward-angle data, which specifically require the inclusion of the MM interaction if they are to be described properly. We will show that mainly because of these data (and the measurements that are in progress) the MM interaction cannot be neglected in a phase-shift analysis of the low-energy $np$ scattering data.

In the present paper, we give the details of our way of including the MM interaction in the $np$ and $pp$ phase-shift analyses. Since our calculation of the $np$ MM scattering amplitude is similar to treatments that have already appeared in the literature, we will only briefly review its derivation in Sec. II. The electromagnetic (em) interaction in $pp$ scattering contains the Coulomb and vacuum polarization interaction, as well as the MM interaction. The corresponding scattering amplitudes are calculated in CDWBA, properly accounting for Coulomb distortion effects. The scattering amplitudes for the Coulomb and vacuum-polarization interactions are well known, and the details of the calculation of the MM scattering amplitude in case of $pp$ scattering are given in Sec. III. Because of this separate treatment of the em scattering amplitude the remaining, i.e., nuclear part, of the amplitude has to be adjusted. This is explained in detail in Sec. IV. Some approximations for including the MM interaction in phase-shift analyses which have appeared in the literature are discussed in Sec. V. The results on the analysis of the $pp$ and $np$ scattering data using our treatment are presented in Sec. VI.

## II. np SCATTERING AMPLITUDE

The most general expression of the nucleon-nucleon scattering amplitude matrix $M$ in the spin-space of the two nucleons, which is invariant under rotations, reflections, and time reversal, can be written as [23,24]

$$M(\mathbf{k}_f, \mathbf{k}_i) = \tfrac{1}{2}\left[\, (a+b) + (a-b)(\boldsymbol{\sigma}_1\cdot\hat{\mathbf{n}})(\boldsymbol{\sigma}_2\cdot\hat{\mathbf{n}})\right.$$

$$
\begin{aligned}
&+(c+d)(\boldsymbol{\sigma}_1\cdot\hat{\mathbf{k}})(\boldsymbol{\sigma}_1\cdot\hat{\mathbf{k}})\\
&+(c-d)(\boldsymbol{\sigma}_1\cdot\hat{\mathbf{q}})(\boldsymbol{\sigma}_1\cdot\hat{\mathbf{q}})\\
&+ie(\boldsymbol{\sigma}_1+\boldsymbol{\sigma}_2)\cdot\hat{\mathbf{n}}+if(\boldsymbol{\sigma}_1-\boldsymbol{\sigma}_2)\cdot\hat{\mathbf{n}}]\ ,
\end{aligned}
\tag{1}
$$

where the caret denotes a unit vector. The momentum vectors are defined in terms of initial and final momenta $\mathbf{k}_i$ and $\mathbf{k}_f$ according to

$$
\mathbf{q}=\tfrac{1}{2}(\mathbf{k}_f+\mathbf{k}_i),\quad \mathbf{k}=\mathbf{k}_f-\mathbf{k}_i,\quad \mathbf{n}=\mathbf{k}_i\times\mathbf{k}_f=\mathbf{q}\times\mathbf{k}\ .
$$

The Wolfenstein-like amplitudes $a,\ldots,f$ are complex functions of the energy and the center-of-mass (c.m.) scattering angle. They are real in the case of BA calculations. For that reason we explicitly included a factor $i$ in the last two terms. Our amplitudes $e$ and $f$ are therefore $-i$ times the amplitudes $e$ and $f$ as defined in Refs. [23] and [24]. For identical particle scattering the $f$ amplitude is absent.

The $M$ matrix can also be written in the singlet-triplet representation of the spin-space. Generalizing the notation introduced by Stapp [25], we write

$$
M=\begin{bmatrix}
M_{SS} & M_{ST} & 0 & M_{ST}\\
M_{TS} & M_{11} & M_{10} & M_{1-1}\\
0 & M_{01} & M_{00} & M_{0-1}\\
M_{TS} & M_{-11} & M_{-10} & M_{-1-1}
\end{bmatrix}\ ,
\tag{2}
$$

with

$$
\begin{aligned}
&M_{-1-1}=M_{11},\ M_{0-1}=-M_{01},\ M_{TS}=-M_{ST},\\
&M_{-11}=M_{1-1},\ M_{-10}=-M_{10}\ .
\end{aligned}
$$

The coefficients of Eq. (1) are related to those of Eq. (2) according to

$$
\begin{aligned}
a&=M_{11}+M_{00}-M_{1-1})/2,\\
b&=M_{11}+M_{SS}+M_{1-1})/2,\\
c&=M_{11}-M_{SS}+M_{1-1})/2,\\
d&=M_{10}+M_{01})/(\sqrt{2}\sin\theta),\\
e&=M_{10}-M_{01})/\sqrt{2},\\
f&=\sqrt{2}M_{ST},
\end{aligned}
\tag{3}
$$

where $\theta$ denotes the c.m. scattering angle.

Still different but equivalent parametrizations of the $M$ matrix have appeared in the literature. For a discussion of the definitions and properties of these various amplitude systems and a tabulation of the transformation matrices among them, we refer to a recent paper by Moravcsik, Pauschenwein, and Goldstein [26]. In the following we will restrict ourselves to what these authors refer to as the Saclay system [Eq. (1)] and the singlet-triplet system [Eq. (2)].

The lowest-order contribution of the em interaction to the nucleon-nucleon scattering amplitude can be obtained from the phenomenological interaction Lagrangian

$$\mathcal{L}_V = ieF_1\overline{\psi}\gamma^\mu\psi A_\mu + \tfrac{1}{2}eF_2\overline{\psi}\sigma^{\mu\nu}\psi(\partial_\mu A_\nu - \partial_\nu A_\mu) \ ,$$

where $\sigma^{\mu\nu} = [\gamma^\mu, \gamma^\nu]/2i$, $A_\mu$ is the photon field, and $\psi$ is the nucleon field. The first term is the usual interaction between the charge $e$ of a nucleon with the em field of the partner nucleon, whereas the second term is the Pauli term describing the interaction of the anomalous magnetic moment with the field. $F_1$ and $F_2$ are the Dirac and Pauli form factors, respectively.

We take the incident nucleon to be the neutron. The one-photon-exchange $np$ scattering matrix is then given by

$$\begin{aligned} M^\gamma_{np} = {} & \frac{\alpha}{2t\sqrt{s}}\left[\overline{u}(n')(F_1^n\gamma^\mu + F_2^n\sigma^{\mu\nu}k_\nu)u(n)\right] \\ & \times \left[\overline{u}(p')[F_1^p\gamma_\mu - F_2^p\sigma_{\mu\nu}k^\nu)u(p)\right] \ , \end{aligned} \tag{4}$$

where $n, p$ and $n', p'$ are the neutron and proton initial and final four-momenta, respectively, and $u(n)$ and $u(p)$ are the Dirac spinors for the neutron and proton. The four-momentum transfer is denoted by $k^\mu = n'^\mu - n^\mu$. Here we have also introduced $\alpha = e^2/4\pi$ and the Mandelstam invariants $s$, $t$ (and $u$) are given by

$$s = -(n+p)^2, \ t = -(n'-n)^2, \ u = -(n'-p)^2 \ . \tag{5}$$

With these definitions the one-photon-exchange $M$-matrix $M^\gamma_{np}$ can be calculated in a straightforward way. Explicit expressions for the one-photon-exchange Wolfenstein-like amplitudes $a, \ldots, f$ have appeared in the literature [27,28] and we reproduce them here for completeness:

$$\begin{aligned} a^\gamma(s,t) = {} & \frac{\alpha}{t\sqrt{s}}\Bigg((F_1^nF_1^p + tF_2^nF_2^p)\Big[s - M_n^2 - M_p^2 + \frac{t}{8sk^2}\Big\{[s-(M_n+M_p)^2][3s-(M_n-M_p)^2] \\ & \qquad + 2[s-(M_n-M_p)^2](\sqrt{s}-M_n-M_p)^2\Big\} \\ & \qquad + \frac{t^2}{16sk^4}[s-(M_n-M_p)^2](\sqrt{s}-M_n-M_p)^2\Big] \\ & + (F_1^nF_1^p + F_2^nF_2^p)t\Big[2\sqrt{s} - M_n - M_p + \frac{t}{2k^2}(\sqrt{s}-M_n-M_p)\Big]\Bigg) \ , \\ b^\gamma(s,t) = {} & \frac{\alpha}{t\sqrt{s}}\Bigg((F_1^nF_1^p - tF_2^nF_2^p)\Big[s - M_n^2 - M_p^2 + \frac{t}{8sk^2}[s+(M_n-M_p)^2][s-(M_n+M_p)^2]\Big] \\ & + (F_1^nF_1^p + F_2^nF_2^p)t(M_n - M_p)\Bigg) \ , \\ c^\gamma(s,t) = {} & \frac{\alpha}{2\sqrt{s}}(F_1^n + 2M_nF_2^n)(F_1^p + 2M_pF_2^p) \ , \\ d^\gamma(s,t) = {} & -c^\gamma(s,t) \ , \\ e^\gamma(s,t) = {} & \frac{-\alpha\sin\theta}{t\sqrt{s}}\Bigg((F_1^nF_1^p + tF_2^nF_2^p)\Big[s - M_n^2 - M_p^2 - \frac{M_n+M_p}{2\sqrt{s}}[s-(M_n-M_p)^2] + \frac{\sqrt{s}-M_n-M_p}{\sqrt{s}+M_n+M_p}\frac{t}{2}\Big] \end{aligned}$$

$$+(F_1^nF_2^p+F_2^nF_1^p)[2k^2\sqrt{s}+t(\sqrt{s}-M_n-M_p)]\Big) \ ,$$

$$f^\gamma(s,t)=\frac{\alpha\sin\theta}{2ts}\left\{(F_1^nF_1^p-tF_2^nF_2^p)(M_n-M_p)[s-(M_n+M_p)^2]+4k^2s(F_1^nF_2^p-F_2^nF_1^p)\right\} \ , \qquad (6)$$

where

$$k^2=[s-(M_n+M_p)^2]\,[s-(M_n-M_p)^2]/4s$$

is the c.m. three-momentum squared.

The Dirac and Pauli form factors $F_1$ and $F_2$ can be expressed in terms of the electric and magnetic Sachs form factors $G_E$ and $G_M$ according to

$$F_1^p=\frac{G_E^p+\tau^pG_M^p}{1+\tau^p}, \quad F_2^p=\frac{G_M^p-G_E^p}{2M_p(1+\tau^p)} \ , \qquad (7)$$

where $\tau^p=-t/4M_p^2$, and similar expressions for the neutron form factors $F_1^n$ and $F_2^n$. For the momentum dependence of the Sachs electric proton form factor $G_E^p$ we use the result of the dipole fit by Hofstadter *et al.* [29],

$$G_E^p(t)=(1-t/M_D^2)^{-2} \ , \qquad (8)$$

with $M_D^2=0.71$ (GeV/$c$)$^2$ the "dipole" mass squared. The magnetic form factors are given by the form factor scaling law

$$G_E^p=\frac{G_M^p}{\mu_p}=\frac{G_M^n}{\mu_n} \ ,$$

with $\mu_p$ and $\mu_n$ the proton and neutron total magnetic moments, respectively. For the neutron electric form factor we choose

$$G_E^n=-\tau^nG_M^n \ ,$$

so $F_1^n(t)\equiv 0$, expressing the fact that the neutron has no charge. In this case only the magnetic moments contribute to the one-photon-exchange amplitude, and we will henceforth refer to the $np$ one-photon-exchange amplitude as the MM amplitude. Different choices for $G_E^n$ can be made [see, e.g., Ref. [30], where $G_E^n=-\tau^nG_M^n/(1+4\tau^n)$ such that only $F_1^n(t=0)=0$], but these only introduce unnecessary algebraic complications. These alternative choices have absolutely no influence in the energy range that will be considered here. For a discussion of various possibilities for the momentum dependence of the electric and magnetic form factors we refer to the literature on electron scattering on protons and deuterons [30,31]. When we neglect the momentum dependence of the form factors we retain the point particle approximation

$$F_1^p=1, \quad F_1^n=0, \quad F_2^p=\frac{\kappa_p}{2M_p}, \quad F_2^n=\frac{\kappa_n}{2M_n} \ , \qquad (9)$$

where $\kappa_p=\mu_p-1=1.792\,847$ and $\kappa_n=\mu_n=-1.913\,043$ are the anomalous proton and neutron magnetic moments, respectively.

Substituting $t = -2k^2(1-\cos\theta)$, we can make a partial-wave decomposition of the $M$-matrix elements, from which the $np$ MM phase shifts can be obtained. The partial-wave $M$ matrix is related to the partial-wave $S$ matrix according to $M \sim (S-1)$. Here we use a symbolic notation and drop all details of spin dependence. The explicit formulas for the decomposition of the $M$ matrix in terms of the partial-wave $S$-matrix elements, including all spin dependence, are well known and detailed expressions can be found, e.g., in Table II of Ref. [32]. Because of the presence of the amplitude $f$ in the MM $np$ scattering amplitude, the $S$ matrix in this case must include spin-singlet spin-triplet transitions. Next to the familiar nuclear bar phase-shift decomposition [33] of the partial-wave spin-triplet coupled $S$ matrix with total angular momentum $J$,

$$S^J_{1,1} = \begin{bmatrix} e^{2i\delta_{J-1,J}}\cos 2\epsilon_J & ie^{i(\delta_{J-1,J}+\delta_{J+1,J})}\sin 2\epsilon_J \\ ie^{i(\delta_{J-1,J}+\delta_{J+1,J})}\sin 2\epsilon_J & e^{2i\delta_{J+1,J}}\cos 2\epsilon_J \end{bmatrix} , \tag{10}$$

we therefore now also have a coupled spin-singlet spin-triplet $S$ matrix with $l = J$:

$$S^J_{0,1} = \begin{bmatrix} e^{2i\delta_l}\cos 2\gamma_l & ie^{i(\delta_l+\delta_{l,l})}\sin 2\gamma_l \\ ie^{i(\delta_l+\delta_{l,l})}\sin 2\gamma_l & e^{2i\delta_{l,l}}\cos 2\gamma_l \end{bmatrix} , \tag{11}$$

where $\gamma_l$ is the nuclear bar spin-flip mixing angle as introduced by Gersten [34,35]. The indices 0 and 1 denote spin singlet and spin triplet, respectively. In this way the partial-wave decomposition of the MM scattering amplitude defines the $np$ MM phase shifts and mixing parameters.

## III. pp SCATTERING AMPLITUDE

The BA one-photon-exchange amplitude in case of $pp$ scattering can easily be obtained from Eq. (6) by replacing neutron form factors and masses by proton form factors and masses, and antisymmetrizing the result. The antisymmetrization comes down to the substitutions

$$\begin{aligned}
a^\gamma(s,t) &\to a^\gamma(s,t) - a^\gamma(s,u), \\
b^\gamma(s,t) &\to b^\gamma(s,t) - c^\gamma(s,u), \\
c^\gamma(s,t) &\to c^\gamma(s,t) - b^\gamma(s,u), \\
d^\gamma(s,t) &\to d^\gamma(s,t) + d^\gamma(s,u), \\
e^\gamma(s,t) &\to e^\gamma(s,t) + e^\gamma(s,u), \\
f^\gamma(s,t) &\to 0 \ .
\end{aligned} \tag{12}$$

However, as was already pointed out by Knutson and Chiang [8], one should use the Coulomb distorted-wave BA rather than the plane-wave BA in case of $pp$ scattering. Breit has argued [3] that the effect of this Coulomb distortion can be approximated reasonably well by multiplying the BA scattering amplitudes with a factor which is now generally referred to as the Breit factor:

$$
\begin{aligned}
M(t) &\rightarrow M(t) e^{-i\eta \ln(1/2)(1-\cos\theta)} , \\
M(u) &\rightarrow M(u) e^{-i\eta \ln(1/2)(1+\cos\theta)} .
\end{aligned}
\tag{13}
$$

The plus or minus sign in front of the $\cos\theta$ term in the Breit factors is prescribed by the $t$ or $u$ dependence of the amplitude, since $t = -2k^2(1-\cos\theta)$ and $u = -2k^2(1+\cos\theta)$. The Coulomb parameter $\eta$ is defined according to [3]

$$
\eta = \frac{\alpha}{v_{\rm lab}} = \frac{M_p \alpha'}{2k} ,
$$

where

$$
\alpha' = \alpha \left(1 + \frac{2k^2}{M_p^2}\right) \left(1 + \frac{k^2}{M_p^2}\right)^{-1/2} .
$$

The employment of the Breit factor represents the main part of the effect of the Coulomb distortion on the scattering amplitude. This can be understood as follows. The pure Coulomb part of the BA $pp$ one-photon-exchange potential only contributes to the diagonal $M$-matrix elements. In the point particle approximation these are given by

$$
\begin{aligned}
M^c_{SS}(t) = M^c_{11}(t) &= M^c_{00}(t) \\
&= M^c_{-1-1}(t) \\
&= \frac{M_p \alpha'}{t} \\
&= -\frac{\eta}{k} \frac{1}{1-\cos\theta} ,
\end{aligned}
$$

all other $M$-matrix elements being zero, and a similar expression for the $u$-dependent amplitudes. The superscript $C$ indicates that we restrict ourselves to the pure Coulomb part. Multiplying with the Breit factors results in

$$
\begin{aligned}
M^c_{SS}(t) = M^c_{11}(t) &= M^c_{00}(t) \\
&= M^c_{-1-1}(t) \\
&= -\frac{\eta}{k} \frac{e^{-i\eta \ln(1/2)(1-\cos\theta)}}{1-\cos\theta} ,
\end{aligned}
\tag{14}
$$

and the same expression with $(1+\cos\theta)$ for the $u$-dependent elements. The result (14) is the exact expression for the Coulomb amplitude in the various spin states. The employment of the Breit factors in the remaining part of the one-photon-exchange $M$-matrix elements has not been justified by explicit calculations, but it fairly well reproduces the $\eta$ dependence as obtained from a consideration of small-angle scattering in the laboratory system [3,6]. The Breit way of including the effect of the Coulomb distortion in the $pp$ one-photon-exchange scattering amplitude is found to be a remarkable good approximation when compared with the exact calculation which will be discussed next.

In order to be able to calculate the $pp$ MM scattering amplitude in CDWBA, we need to know the MM potential in coordinate space. The $pp$ em potential in coordinate space, containing the MM potential, can best be calculated by also taking into account the planar and crossed box two-photon-exchange diagrams. This potential then gives the proper lowest-order relativistic and recoil corrections for the scattering amplitude, phase shifts, and bound-state energies, when it is inserted in the relativistic Schrödinger equation [36,37]. One should realize that the relativistic Schrödinger equation is nothing else but a differential form of the relativistic Lippmann-Schwinger equation, which in turn is totally equivalent with three-dimensional integral equations such as the Blankenbecler-Sugar-Logunov-Tavkhelidze equation [38]. The details of the derivation of this improved Coulomb potential are given elsewhere [39,40]. Its long-range part is given by

$$V_{\rm em}(r) = V_{C1}(r) + V_{C2}(r) + V_{\rm MM}(r) + V_{\rm VP}(r) \ , \tag{15}$$

with $V_{C1}$ the point-charge Coulomb potential, $V_{C2}$ the relativistic correction to this potential, $V_{\rm MM}$ the magnetic moment potential, and $V_{\rm VP}$ the vacuum-polarization potential as derived by Uehling [41] and reviewed by Durand [42]. Explicit expressions for these $pp$ potentials are

$$\begin{aligned}
V_{C1}(r) &= \tfrac{\alpha'}{r}, \\
V_{C2}(r) &= -\tfrac{1}{2M_p^2}\left[(\Delta+k^2)\tfrac{\alpha}{r} + \tfrac{\alpha}{r}(\Delta+k^2)\right] \\
&\approx -\tfrac{\alpha\alpha'}{M_p r^2}, \\
V_{\rm MM}(r) &= f_T \tfrac{S_{12}}{r^3} + f_{LS}\tfrac{\mathbf{L}\cdot\mathbf{S}}{r^3}, \\
V_{\rm VP}(r) &= \tfrac{2\alpha}{3\pi}\tfrac{\alpha'}{r}\int_1^\infty dx e^{-2m_e r x}\left[1+\tfrac{1}{2x^2}\right]\tfrac{(x^2-1)^{1/2}}{x^2},
\end{aligned} \tag{16}$$

with $S_{12} = 3(\boldsymbol{\sigma}_1\cdot\hat{\mathbf{r}})(\boldsymbol{\sigma}_2\cdot\hat{\mathbf{r}}) - (\boldsymbol{\sigma}_1\cdot\boldsymbol{\sigma}_2)$ the tensor operator, $\Delta$ the Laplacian, $m_e$ the electron mass, and

$$f_T = -\frac{\alpha}{4M_p^2}\mu_p^2, \quad f_{LS} = -\frac{\alpha}{4M_p^2}\left(6+8\kappa_p\right) \ . \tag{17}$$

The $1/r^2$ dependence of the relativistic Coulomb potential can be understood as follows. From the solution of the radial Schrödinger equation

$$(\Delta + k^2)F_l(\eta, r) = M_p V_{C1}(r) F_l(\eta, r) \ ,$$

with $F_l(\eta, r)$ the regular Coulomb function, it follows that in the CDWBA the operator $\Delta + k^2$ is equivalent to $M_p V_{C1}(r) = M_p\alpha'/r$. So in the CDWBA the potential $V_{C2}(r)$ is equivalent to $-\alpha\alpha'/M_p r^2$. The contributions of the relativistic Coulomb and vacuum-polarization potentials to the scattering amplitude have been discussed elsewhere [10,42], and so we will here restrict ourselves to the contribution of the MM potential.

With the $pp$ MM potential in coordinate space, $V_{\rm MM}(r)$, we can define the partial-wave MM $K$ matrix according to

$$K^{\rm MM}(l,l') = -\frac{M_p}{k}\int_0^\infty dr F_l(\eta,r)V_{\rm MM}(r)F_{l'}(\eta,r) \ . \tag{18}$$

The $1/r^3$ dependence of the potential and the presence of the tensor operator, which couples states with $J=l+1=l'-1$, lead to integrals of the type

$$I_{l,l'} = k^{-2}\int_0^\infty dr F_l(\eta,r)F_{l'}(\eta,r)r^{-3} \ , \tag{19}$$

where [43]

$$\begin{aligned} I_{l,l} &= \frac{1}{2l(l+1)} \\ &\quad + \frac{1-\pi\eta+\pi\eta\coth\pi\eta - 2\eta^2\sum_{n=0}^{l}(n^2+\eta^2)^{-1}}{2l(l+1)(2l+1)} \ , \\ I_{l,l+2} &= \frac{1}{6}|l+1+i\eta|^{-1}|l+2+i\eta|^{-1} \ . \end{aligned} \tag{20}$$

In analogy with Stapp [32] we introduce a short-hand notation for the spin and angular momentum states of the $K$-matrix elements. The spin-singlet state with $l=J$ is denoted by $K_l$ and the spin-triplet states are denoted by $K_{l,J}$, where $J=l-1,l,l+1$. The off-diagonal element of the spin-triplet coupled state with $J=l+1=l'-1$ is denoted by $K_{{\rm off},J}$. The MM potential $V_{\rm MM}$ does not contribute to the spin-singlet $K$-matrix elements, so $K_l^{\rm MM}=0$. The uncoupled $l=J$ spin-triplet MM $K$-matrix elements are given by

$$K_{l,l}^{\rm MM} = -M_p k\left(2f_T - f_{LS}\right) I_{l,l} \ , \tag{21}$$

whereas the elements of the triplet coupled MM $K$ matrix with total angular momentum $J$ are given by

$$\begin{aligned} K_{l,l+1}^{\rm MM} &= -M_p k\left[\frac{-2l}{2l+3}f_T + l f_{LS}\right] I_{l,l} \ , \\ K_{l+2,L+1}^{\rm MM} &= -M_p k\left[-\frac{2l+6}{2l+3}f_T - (l+3)f_{LS}\right] I_{l+2,l+2} \ , \\ K_{{\rm off},J}^{\rm MM} &= K_{{\rm off},l}^{\rm MM} \\ &= -M_p k\left[6\frac{\sqrt{(l+1)(l+2)}}{2l+3}f_T\right] I_{l,l+2} \ . \end{aligned} \tag{22}$$

Next we construct the partial wave $R$ matrix which is defined by $R=S-1=2iK(1-iK)^{-1}$. These MM $R$-matrix elements have to be adjusted according to

$$R(l,l') \to e^{i\sigma_l}R(l,l')e^{i\sigma_{l'}} \ , \tag{23}$$

with $\sigma_l = \arg\Gamma(l+1+i\eta)$ the Coulomb phase shifts. This adjustment will be explained in more detail in the next section.

The $pp$ MM phase shifts are now readily obtained using the nuclear bar phase-shift decomposition of the $S$ matrix. For the spin-singlet and spin-triplet uncoupled states we have $S = e^{2i\delta_l}$ and $S = e^{2i\delta_{l,l}}$, respectively, whereas for the coupled states we use Eq. (10). The spin-flip mixing angle as introduced in Eq. (11) equals zero because we are considering identical particle scattering, i.e., $\gamma_l(pp) = 0$.

Finally, the *pp* MM scattering amplitude is obtained by summing the partial-wave $R$-matrix elements with Legendre polynomials. Explicit expressions for these summation formulas can be found, e.g., in Table II of Ref [32]. The summation can be done term by term on a computer and in our calculations we include all partial waves up to $l = 1000$. However, substituting the MM $R$-matrix elements in the summation formulas for $M_{10}$ and $M_{01}$, the $1/2l(l+1)$ part in $I_{l,l}$ is seen to give rise to a contribution

$$Z_{LS} = -\frac{M_p}{\sqrt{2}} f_{LS} \sum_{\text{odd } l} e^{2i(\sigma_l - \sigma_0)} \frac{2l+1}{l(l+1)} P_l^1(\theta) \tag{24}$$

to $M_{10}$, and the same contribution with a plus sign to $M_{01}$. This expression converges much too slowly for a summation on a computer to be practical. Fortunately, it can be handled analytically (see also Ref. [8]), resulting in

$$\begin{aligned} Z_{LS} = -\frac{M_p f_{LS}}{\sin\theta\sqrt{2}} \Big( & e^{-i\eta \ln(1/2)(1-\cos\theta)} \\ & + e^{-i\eta \ln(1/2)(1+\cos\theta)} - 1 \Big) \ . \end{aligned} \tag{25}$$

In our computations, this analytical result was used. It is obtained as follows. Using the expression for the Coulomb phase shifts

$$e^{2i\sigma_l} = \frac{\Gamma(l+1+i\eta)}{\Gamma(l+1-i\eta)}$$

and the recurrence relations for the Legendre polynomials, we have

$$\begin{aligned} \sin\theta \sum_{\text{odd } l} & e^{2i(\sigma_l-\sigma_0)} \frac{2l+1}{l(l+1)} P_l^1(\theta) \\ &= \sum_{\text{odd } l} e^{2i(\sigma_l-\sigma_0)} [P_{l-1}(\theta) - P_{l+1}(\theta)] \\ &= \sum_{\text{even } l} \frac{2l+1}{2} \frac{4i\eta e^{2i(\sigma_l-\sigma_0)}}{(l+1-i\eta)(l+i\eta)} P_l(\theta) \ - \ 1 \ . \end{aligned}$$

With the help of Eq. (7.127) of Gradshteyn and Ryzhik [44] we then find

$$\begin{aligned} \sum_{\text{odd } l} e^{2i(\sigma_l-\sigma_0)} \frac{2l+1}{l(l+1)} P_l^1(\theta) &= \frac{1}{\sin\theta} \\ \times \Big( e^{-i\eta \ln(1/2)(1-\cos\theta)} &+ e^{-i\eta \ln(1/2)(1+\cos\theta)} - 1 \Big) \ . \end{aligned}$$

It is important to note that the result (25) cannot be obtained by multiplying the corresponding BA amplitude with the Breit factors.

A remark on the effect of the form factors on the MM scattering amplitude is in order here. The short-range part of the MM potential is more complicated than the expression given in Eq. (16). In the point particle approximation of Eq. (9), there are additional contact terms. These contact terms only contribute to the MM $K$-matrix elements for $J = 0$ and 1. Taking into account the momentum dependence of the form factors as in Eq. (8), the contact terms are replaced by Yukawa-like potentials. The contributions of these Yukawa-like potentials to the $K$-matrix integral of Eq. (18) can be calculated accurately in a fast and elegant way using recurrence relations [45]. They are only of importance in the lowest partial waves ($l \lesssim 2$ in the 0–30-MeV analyses and $l \lesssim 4$ in the 0–350-MeV analyses). We do not find any significant differences in the results of our phase-shift analyses when we replace the form factors of Eq. (8) by their point particle approximation (9). This is not surprising in view of the short-range effect of the contact terms and the fact that the lower partial waves in our analyses are parametrized.

## IV. ELECTROMAGNETIC CORRECTIONS TO THE NUCLEAR AMPLITUDE

The total scattering amplitude can be separated into a purely electromagnetic (em) part and a nuclear part. The nuclear part of the amplitude contains nuclear phase shifts, which are phase shifts with respect to em wave functions.

First, we will discuss the separation of the $np$ amplitude. In that case the em potential only consists of the MM interaction. The scattering amplitude for the long-range MM potential and the corresponding MM phase shifts are given in Sec. II. The partial-wave phase shift $\delta_{\mathrm{MM}+N}$ of the long-range MM potential plus the short-range nuclear potential, can be decomposed into a phase shift $\delta^{\mathrm{MM}}_{\mathrm{MM}+N}$ of the MM plus nuclear interaction with respect to the MM wave functions, and the phase shift $\delta_{\mathrm{MM}}$ of the MM interaction itself, i.e.,

$$\delta_{\mathrm{MM}+N} = \delta^{\mathrm{MM}}_{\mathrm{MM}+N} + \delta_{\mathrm{MM}} \ . \tag{26}$$

For coupled channels this addition law has to be translated into a multiplication law for $S$ matrices:

$$S_{\mathrm{MM}+N} = (S_{\mathrm{MM}})^{1/2} S^{\mathrm{MM}}_{\mathrm{MM}+N} (S_{\mathrm{MM}})^{1/2} \ , \tag{27}$$

where the adjustment factor $S^{1/2} = (1 + K^2)^{1/2}(1 - iK)^{-1}$ is well-defined since the first factor, the square root of a positive definite matrix, is uniquely defined. The generalization to additional potentials is obvious [see Eq. (34)].

Neglecting for a moment all details of spin dependence, the $np$ total scattering amplitude is given by

$$M_{\mathrm{MM}+N}(\theta) = \frac{1}{2ik} \sum_l (2l+1)(e^{2i\delta_{\mathrm{MM}+N,l}} - 1) P_l(\theta) \ . \tag{28}$$

Using the phase-shift decomposition of Eq. (26), we have

$$\begin{aligned} \left(e^{2i\delta_{\mathrm{MM}+N}} - 1\right) = & \left(e^{2i\delta_{\mathrm{MM}}} - 1\right) \\ & + e^{i\delta_{\mathrm{MM}}} \left(e^{2i\delta^{\mathrm{MM}}_{\mathrm{MM}+N}} - 1\right) e^{i\delta_{\mathrm{MM}}} \ , \end{aligned} \tag{29}$$

and the total scattering amplitude can be written as

$$M_{\mathrm{MM}+N}(\theta) = M_{\mathrm{MM}}(\theta) \ + M^{\mathrm{MM}}_{\mathrm{MM}+N}(\theta) \ , \tag{30}$$

where

$$M_{\mathrm{MM}}(\theta) = \frac{1}{2ik}\sum_{l}(2l+1)\left(e^{2i\delta_{\mathrm{MM},l}}-1\right)P_l(\theta) \tag{31}$$

and

$$\begin{aligned} M^{\mathrm{MM}}_{\mathrm{MM}+N}(\theta) = \frac{1}{2ik}\sum_{l}\,&(2l+1)e^{i\delta_{\mathrm{MM},l}}\left(e^{2i\delta^{\mathrm{MM}}_{\mathrm{MM}+N,l}}-1\right) \\ &\times e^{i\delta_{\mathrm{MM},l}}P_l(\theta) \end{aligned} \tag{32}$$

represent the MM scattering amplitude, and the nuclear amplitude of the MM plus nuclear interaction with respect to MM wave functions, respectively. Of course, for coupled channels the appropriate decomposition in terms of $S$ matrices must be used. The reason for the decomposition of Eq. (30) is that the slowly converging series of Eq. (28) is split into a slowly converging series (31) for the MM amplitude $M_{\mathrm{MM}}$, which can be summed exactly, and a much faster converging series (32) for the nuclear amplitude $M^{\mathrm{MM}}_{\mathrm{MM}+N}$. The correct spin-dependent expressions for $M_{\mathrm{MM}}$ are given in Sec. II. The series (32) for the nuclear amplitude is so rapidly converging because of the short range of the nuclear interaction. This causes the phase shifts $\delta^{\mathrm{MM}}_{\mathrm{MM}+N}$, due to the short-range nuclear potential, to approach zero rapidly for increasing orbital angular momentum $l$ and therefore only a limited number of terms is needed in the summation.

It is important to note that the partial-wave nuclear amplitudes must be adjusted with factors $e^{i\delta_{\mathrm{MM}}}$ or, in case of coupled channels, with factors $(S_{\mathrm{MM}})^{1/2}$. Without this adjustment the nuclear phase shifts $\delta^{\mathrm{MM}}_{\mathrm{MM}+N}$ are not properly separated from the MM phase shifts $\delta_{\mathrm{MM}}$. The nuclear phase shifts $\delta^{\mathrm{MM}}_{\mathrm{MM}+N}$ are usually used to parametrize the nuclear scattering amplitude in a phase-shift analysis.

For $pp$ scattering the construction of the total amplitude is more complicated, because now the em potential consists of the four terms given by Eqs. (15) and (16). The decomposition analogs to Eqs. (26) and (27) are

$$\begin{aligned} \delta_{\mathrm{em}+N} = \delta_{C1} &+ \delta^{C1}_{C1+C2} + \delta^{C1+C2}_{C1+C2+\mathrm{MM}} \\ &+\delta^{C1+C2+\mathrm{MM}}_{C1+C2+\mathrm{MM}+\mathrm{VP}} + \delta^{\mathrm{em}}_{\mathrm{em}+N} \ , \end{aligned} \tag{33}$$

and

$$\begin{aligned} S_{\mathrm{em}+N} = (S_{C1})^{1/2}&(S^{C1}_{C1+C2})^{1/2}(S^{C1+C2}_{C1+C2+\mathrm{MM}})^{1/2} \\ &\times(S^{C1+C2+\mathrm{MM}}_{C1+C2+\mathrm{MM}+\mathrm{VP}})^{1/2}S^{\mathrm{em}}_{\mathrm{em}+N} \\ &\times(S^{C1+C2+\mathrm{MM}}_{C1+C2+\mathrm{MM}+\mathrm{VP}})^{1/2}(S^{C1+C2}_{C1+C2+\mathrm{MM}})^{1/2} \\ &\times(S^{C1}_{C1+C2})^{1/2}(S_{C1})^{1/2} \ . \end{aligned} \tag{34}$$

The left-right multiplications of $S^{\mathrm{em}}_{\mathrm{em}+N}$ with the square root $S$ matrices of the different parts of the em interaction are in order of increasing range of these parts. So the $S$ matrix of the exponential vacuum polarization is closest to the center of Eq. (34), followed by the $S$ matrix of the $1/r^3$ MM potential and the $S$ matrix of the $1/r^2$ relativistic Coulomb potential. The final left-right multiplication is with the $S$ matrix of the longest-range $1/r$ Coulomb potential. The tensor nature of the MM interaction makes it such that the MM $S$ matrix in the triplet coupled channels is nondiagonal, and so the order of multiplication is important.

The MM interaction as well as the vacuum-polarization interaction are usually only treated in CDWBA (except perhaps for $l = 0$). This means that we make the approximations

$$\begin{aligned} S^{C1+C2}_{C1+C2+\mathrm{MM}} &\approx S^{C1}_{C1+\mathrm{MM}}, \\ S^{C1+C2+\mathrm{MM}}_{C1+C2+\mathrm{MM}+\mathrm{VP}} &\approx S^{C1}_{C1+\mathrm{VP}} . \end{aligned} \tag{35}$$

The corresponding phase shifts are

$$\delta_{\mathrm{em}+N} \approx \sigma_l + \rho_l + \phi_l + \tau_l + \delta^{\mathrm{em}}_{\mathrm{em}+N} , \tag{36}$$

where

$$\begin{aligned} \delta_{C1} &\equiv \sigma_l = \arg \Gamma(l+1+i\eta), \\ \delta^{C1}_{C1+C2} &\equiv \rho_l \approx \tfrac{\alpha\alpha'}{2l+1}\left[\tfrac{\pi}{2} - \tfrac{d\sigma_l}{dl}\right], \\ \delta^{C1+C2}_{C1+C2+\mathrm{MM}} &\approx \delta^{C1}_{C1+\mathrm{MM}} \equiv \phi_l, \\ \delta^{C1+C2+\mathrm{MM}}_{C1+C2+\mathrm{MM}+\mathrm{VP}} &\approx \delta^{C1}_{C1+\mathrm{VP}} \equiv \tau_l, \end{aligned} \tag{37}$$

and $\delta^{\mathrm{em}}_{\mathrm{em}+N}$ is the phase shift of the em plus nuclear potential with respect to em wave functions. The phase shifts $\rho_l$ of the relativistic Coulomb potential are given in Ref. [40], the MM phase shifts $\phi_l$ were derived in the previous section, and expressions for the vacuum-polarization phase shifts $\tau_l$ can be found in the papers by Durand [42] and Gursky and Heller [46]. Exact expressions for these phase shifts including the effects of the relativistic Coulomb and MM interaction, i.e., $\delta^{C1+C2}_{C1+C2+\mathrm{MM}}$ and $\delta^{C1+C2+\mathrm{MM}}_{C1+C2+\mathrm{MM}+\mathrm{VP}}$, are not known to us. In practice, the aforementioned approximations suffice for all partial waves, except perhaps for $l = 0$. Therefore, for $l > 0$ we use $\phi_l$ and $\tau_l$, whereas for the ${}^1S_0$ partial wave the explicit phase shift $\delta^{C1+C2+\mathrm{MM}}_{C1+C2+\mathrm{MM}+\mathrm{VP}}$ is used (for details, see Ref. [10]). We do not have to include the MM contribution $\delta^{C1+C2}_{C1+C2+\mathrm{MM}}$ to this phase shift, because the long-range part of the MM interaction does not contribute in the spin-singlet partial waves.

With the approximated phase-shift decomposition of Eq. (36) we can now also split up the *pp* total scattering amplitude. For convenience we make the next approximation, which is sufficiently accurate in practical calculations:

$$\begin{aligned} (S_{\mathrm{em}+N} - 1) = {} & \left(e^{2i\sigma_l} - 1\right) + e^{i\sigma_l}\left(e^{2i\rho_l} - 1\right)e^{i\sigma_l} + e^{i\sigma_l}\left(S^{C1}_{C1+\mathrm{MM}} - 1\right)e^{i\sigma_l} + e^{i\sigma_l}\left(e^{2i\tau_l} - 1\right)e^{i\sigma_l} \\ & + e^{i(\sigma_l+\rho_l)}\left(S^{C1}_{C1+\mathrm{MM}}\right)^{1/2} e^{i\tau_l}\left(S^{\mathrm{em}}_{\mathrm{em}+N} - 1\right)e^{i\tau_l}\left(S^{C1}_{C1+\mathrm{MM}}\right)^{1/2} e^{i(\rho_l+\sigma_l)} , \end{aligned} \tag{38}$$

where $S^{\mathrm{em}}_{\mathrm{em}+N}$ contains the phase shifts with respect to the total em interaction. From Eq. (38) it is now clear why the MM $R$-matrix elements defined in the previous section have to be adjusted with factors $e^{i\sigma_l}$ as in Eq. (23). The approximation $e^{i\sigma_l}\left(e^{2i\tau_l}-1\right)e^{i\sigma_l}$ for the contribution to the vacuum-polarization amplitude is made, because this is the way Durand [42] derived his expression for the vacuum-polarization amplitude. Without this approximation the construction of the amplitude is much more difficult. Similarly, the approximation $e^{i\sigma_l}\left(S^{C1}_{C1+\mathrm{MM}}-1\right)e^{i\sigma_l}$ for the contribution of the MM amplitude simplifies the expressions for this amplitude also. For example, we have not been able to find an analytical expression for the slowly converging contribution $Z_{LS}$ of Eq. (25) when we included the relativistic Coulomb phase shifts $\rho_l$ next to the Coulomb phase shifts $\sigma_l$ in the adjustment factors.

From Eq. (38), we find that the $pp$ total scattering amplitude $M_{\mathrm{em}+N}(\theta)$ can be written as

$$\begin{aligned} M_{\mathrm{em}+N}(\theta) = M_{C1}(\theta) + M^{C1}_{C1+C2}(\theta) + M^{C1}_{C1+\mathrm{MM}}(\theta) \\ + M^{C1}_{C1+\mathrm{VP}}(\theta) + M^{\mathrm{em}}_{\mathrm{em}+N}(\theta)\ , \end{aligned} \tag{39}$$

where we neglected details of anti-symmetrization. The amplitudes on the right-hand side are the Coulomb amplitude as given in Eq. (14), the relativistic correction to the Coulomb amplitude [10,40], the magnetic moment amplitude as derived in the previous section, the vacuum-polarization amplitude as given by Durand [42], and the nuclear amplitude, respectively. The nuclear amplitude in terms of $S$ matrices is represented by

$$\begin{aligned} M^{\mathrm{em}}_{\mathrm{em}+N} \sim S^{1/2}_{C1}\ S^{1/2}_{C2}\ S^{1/2}_{\mathrm{MM}}\ S^{1/2}_{\mathrm{VP}}\ \left(S^{\mathrm{em}}_{\mathrm{em}+N}-1\right) \\ \times S^{1/2}_{\mathrm{VP}}\ S^{1/2}_{\mathrm{MM}}\ S^{1/2}_{C2}\ S^{1/2}_{C1}\ , \end{aligned} \tag{40}$$

where the square-root factors are the $S$-matrix versions of the exponential adjustment factors appearing in Eq. (38).

## V. APPROXIMATIONS FOR INCLUDING THE MAGNETIC MOMENT INTERACTION

For $pp$ scattering no analytical expressions for the em scattering amplitude exist, except for the point-particle Coulomb amplitude. The contributions of the relativistic Coulomb, magnetic moment, and vacuum-polarization amplitudes are obtained by summing the corresponding partial-wave amplitudes over a large number of partial waves. An approximation is that the MM and vacuum-polarization amplitudes are calculated with respect to Coulomb wave functions and that the square-root adjustment factors solely contain the Coulomb phase shifts $\sigma_l$. We believe that these approximations are good enough for practical purposes, and we will therefore use them in our $pp$ phase-shift analysis. The exact expressions are much more difficult to obtain, and the differences with the approximations just mentioned are expected to be small.

Other, more crude approximations for including the em interaction in a $pp$ phase-shift analysis have appeared in the literature. In such approximations only the most important parts of the em interaction to the scattering amplitude are retained, considerably simplifying the expressions for the amplitude. These approximations could be made because until recently the scattering data have not been accurate enough for the differences with the more exact treatment to show up clearly and significantly.

The contributions of the relativistic Coulomb and vacuum-polarization potentials are of order $\alpha^2$, and are therefore not included in the phase-shift analyses of Arndt, Hyslop, and Roper [12], and of Bystricky, Lechanoine-Leluc, and Lehar [13]. The importance of the vacuum polarization can be seen explicitly in the low-energy region up to a few MeV. So the effect of the vacuum-polarization interaction has to be accounted for if such low-energy data are to be described properly [9,10,47].

Although the influence of the MM interaction on the scattering amplitude is largest in the lower partial waves, it has been argued by Breit and Ruppel [5] that it is not necessary to include these effects explicitly, because these lower partial-wave phase shifts are parametrized anyway. In this approximation only the Coulomb interaction is included in the adjustment factors for the nuclear amplitude, i.e., Eq. (40) only contains $S_{C1}^{1/2} = e^{i\sigma_l}$, whereas the other square-root $S$ matrices are left out. The MM interaction is, however, included in the higher partial waves.

This approximation is used in the Saclay phase-shift analysis of Bystricky, Lechanoine-Leluc, and Lehar [13], where they calculate the higher partial-wave MM scattering amplitudes for $l > l_{\max}$ in BA. Here $l_{\max} = 5$ denotes the highest partial wave which is parametrized. As a second approximation, they only take account of the spin-orbit part of the MM interaction, neglecting the tensor part. In this approximation the effect of the MM interaction only contributes to the $e$ amplitude of Eq. (1) and is given by

$$\begin{aligned} e_{\mathrm{BA}}^{\mathrm{MM}} &= (M_{10} - M_{01})/\sqrt{2} \\ &= \frac{\alpha}{2M_p}(3 + 4\kappa_p) \\ &\quad \times \left[ \frac{1}{\sin\theta} - \sum_{\text{odd } l}^{l_{\max}} \frac{2l+1}{l(l+1)} P_l^1(\theta) \right] , \end{aligned} \tag{41}$$

where the subscript BA denotes that the amplitude is calculated in BA. This amplitude can also easily be calculated in CDWBA, using Coulomb functions and adjusting with factors $e^{i\sigma_l}$, yielding

$$\begin{aligned} e_{\mathrm{CD}}^{\mathrm{MM}} &= \frac{\alpha}{2M_p}(3 + 4\kappa_p) \\ &\quad \times \left[ \frac{e^{-i\eta\ln(1/2)(1-\cos\theta)} + e^{-i\eta\ln(1/2)(1+\cos\theta)} - 1}{\sin\theta} \right. \\ &\quad \left. \sum_{\text{odd } l}^{l_{\max}} e^{2i(\sigma_l - \sigma_0)} \frac{2l+1}{l(l+1)} P_l^1(\theta) \right) . \end{aligned} \tag{42}$$

where the subscript CD denotes that the amplitude is calculated in CDWBA. The amplitudes $e_{\mathrm{BA}}^{\mathrm{MM}}$ and $e_{\mathrm{CD}}^{\mathrm{MM}}$ correspond to the slowly converging, and therefore most important part $Z_{LS}$ of the $pp$ MM amplitude as given in Eq. (25). We want to point out that the terms $e_{\mathrm{BA}}^{\mathrm{MM}}$ or $e_{\mathrm{CD}}^{\mathrm{MM}}$ suffice as a first approximation for the inclusion of the MM interaction only. They are not sufficient for a proper description of the new high accuracy analyzing power measurements.

Another approximation for including the effects of the MM interaction has already been mentioned in Sec. III. In this treatment the MM scattering amplitude is calculated in BA and approximately corrected for Coulomb distortion effects by employing the Breit factors [3] as given by Eq. (13). This approach is used in the Blacksburg analyses of Arndt *et al.* [11,12]. However, the nuclear amplitude in these analyses is not adjusted for the fact that in that case the MM interaction is included in all partial waves, i.e., they do not include $S^{1/2}_{\rm MM}$ in Eq. (40) either. This approximated treatment of the Coulomb distortion effect and neglect of the MM interaction in the adjustment factors of the nuclear amplitude already gives a very good description of the *pp* scattering data. A similar treatment has been used by Bystricky *et al.* [48] when they investigated the influence of the MM interaction on their *pp* phase-shift analysis. The improvement in the description of the *pp* scattering data was found to be small and could only be seen in a data set that contained all data in a sufficiently large energy range. Nevertheless, the high accuracy of recent *pp* analyzing power experiments makes that the slight differences between this treatment and our more exact treatment have become more pronounced. This has been shown explicitly by us in a separate publication [17].

For *np* scattering the situation is somewhat different. Here the em interaction consists of the MM interaction only, and expressions for the MM scattering amplitude can be calculated analytically. Therefore, there are essentially only two approximations for including the MM interaction in an *np* phase-shift analysis. Next to the inclusion of the MM scattering amplitude in all partial waves, one can either include the $S^{1/2}_{\rm MM}$ factors in the nuclear amplitude (as is done in our analyses), or one can leave them out (as is done in the Blacksburg analyses [11,12]).

## VI. RESULTS

### A. pp analysis

We will first discuss the effects of the MM interaction in our phase-shift analysis of the *pp* scattering data below $T$lab = 350 MeV. The difference with our recently published analysis [49] is that we have here included the new 50.04-MeV $A_y$ data of Smyrski et al. [16]. Our *pp* data base now contains 1636 scattering observables or, including the 130 normalization data, 1766 scattering data. In our analysis we use an energy-dependent $P$-matrix parametrization to parametrize the short-range interaction (see Refs. [10,49]). This $P$ matrix is the logarithmic derivative of the radial wave function at some boundary condition radius $r = b$. The long-range interaction is described by a potential tail. For *pp* scattering the em part of the long-range potential consists of the modified Coulomb potential $V_{C1}+V_{C2}$, the MM potential $V_{\rm MM}$, and the vacuum-polarization potential $V_{\rm VP}$. For the nuclear part of the potential tail, we take the one-pion-exchange (OPE) potential plus the heavy-boson-exchange (HBE) parts of the Nijmegen soft-core *NN* potential [50]. To parametrize the short-range interaction, we use 28 parameters for the lower partial waves with total angular momentum $J \leq 4$. All higher partial waves are given by OPE phase shifts calculated in CDWBA.

In our recently published $pp$ phase-shift analysis [49], the intermediate partial waves ($5 \leq J \leq 8$) are treated differently. There we use the phase shifts of the OPE plus HBE contributions of the Nijmegen $NN$ potential to parametrize these waves. The reason that we here only use the OPE phase shifts in the intermediate partial waves is the following. In one of the treatments for including the MM interaction, the MM interaction is only included in the higher partial waves ($l \geq 5$). It was argued by Breit and Ruppel [5] that in a first approximation the effects of the MM interaction need not be included in the lower partial waves, since they are parametrized anyway. The parameters can largely compensate for any shortcomings which may arise due to the fact that the MM interaction is not included in these lower partial waves. However, when we use the phase shifts of the OPE plus HBE contributions of the Nijmegen potential for the intermediate partial waves, there are no parameters which can compensate for such shortcomings in these waves. A satisfactory fit to the $pp$ data in that case turned out to be impossible.

We compare five different treatments A–E for including the MM interaction in the $pp$ phase-shift analysis. We also define a case F, which is the treatment as used in our 0–350-MeV $pp$ phase-shift analysis [49]; i.e., for the intermediate partial waves with $5 \leq J \leq 8$ we use the phase shifts of the OPE plus HBE contributions of the Nijmegen $NN$ potential, and the MM interaction is included in all partial waves. This treatment gives the best fit to the $pp$ scattering data and is included for completeness. The different treatments A–F are as follows.

(A) No MM interaction at all.

(B) Inclusion of spin-orbit part of the MM scattering amplitude in the higher partial waves with $l > l_{\rm max} = 4$ only, calculated in BA using Eq. (41).

(C) Same as case B, but calculated in the CDWBA using Eq. (42).

(D) Inclusion of MM scattering amplitude in all partial waves, calculated in the BA using Eq. (6) adapted to $pp$ scattering, and approximately corrected for Coulomb distortion effects using the Breit factors as in Eq. (13).

(E) Inclusion of MM scattering amplitude in all partial waves, calculated in the CDWBA by properly accounting for Coulomb distortion effects. Adjustment of the nuclear amplitude according to Eq. (40).

(F) Same as case E, but using the phase shifts of the OPE plus HBE contributions of the Nijmegen $NN$ potential for the intermediate partial waves with $5 \leq J \leq 8$.

In all these cases, the amplitudes of the relativistic Coulomb and vacuum-polarization potentials are taken into account also. Treatment B corresponds to the way the MM interaction is included in the Saclay phase-shift analysis of Bystricky, Lechanoine-Leluc, and Lehar [13]. Treatment D corresponds to the way the MM interaction is included in the Blacksburg phase-shift analyses of Arndt *et al.* [11,12], whereas case E (or more properly case F) corresponds to the Nijmegen treatment.

For $N_{\rm dat} = 1766$ we find the results as given in the first line of Table I. The large rise in $\chi^2_{\rm min}$ for case B is almost totally because of an inadequate description of the forward-angle analyzing power data of Barker *et al.* [51] at 5.05 and 9.85 MeV, and of the data of Hutton *et al.* [7] at 10.0 MeV. This is because the addition of the BA MM scattering amplitude in the higher partial waves (case B) gives rise to a more pronounced dip structure in the analyzing power, which is in disagreement with these experimental data. This is demonstrated in Fig. 1, where we give the results of the four different treatments A, B, D, and E. The experimental data points are the analyzing power data of Barker *et al.* [51] at 5.05 and 9.85 MeV. The more complete treatments D and E give practically the same results as treatment A where the the MM interaction is left out altogether, and all three cases are in excellent agreement with the data. This was already found by Knutson and Chiang [8], who showed that one should use the CDWBA rather than the BA calculation for the MM scattering amplitude.

The Coulomb distortion can easily be incorporated in the spin-orbit part of the higher partial wave MM scattering amplitudes using Eq. (42). Indeed, treatment C gives an enormous improvement when compared to treatment B. Nevertheless, treatment C is still not good enough as a means for including the MM interaction. Inclusion of the MM amplitude in *all* partial waves as in treatments D and E gives an additional improvement of almost 90 in $\chi^2_{\rm min}$. The approximation of treatment D is seen to be just as good as treatment E, which is somewhat surprising in view of the fact that in treatment D the Coulomb distortion effect is only included approximately. Inclusion of the HBE parts of the Nijmegen potential in the intermediate partial waves (treatment F) gives an additional drop of 20 in $\chi^2_{\rm min}$.

Because of the relatively high contribution of the low-energy data to $\chi^2_{\rm min}$ for treatment B, we thought it more proper to compare the different treatments in an analysis where we do not include these low-energy data. We therefore also give the results of the analyses where we do not include data with $T_{\rm lab} \leq 10$ MeV. We are then left with 1431 scattering data, and the results of the various treatments are given in the second line of Table I. We see that now the difference between treatments B and C has almost disappeared, and both treatments give a drop of about 60 in $\chi^2_{\rm min}$ when compared with treatment A. An additional drop of about 55 in $\chi^2_{\rm min}$ is reached when the MM interaction is included in *all* partial waves (treatment D). Still, inclusion of the adjustments to the nuclear amplitude (treatment E) gives a further drop of 10 in $\chi^2_{\rm min}$. And again treatment F gives an additional drop of 20 in $\chi^2_{\rm min}$ and gives the best fit to the data.

As was already mentioned in the Introduction, the influence of the MM interaction on the description of the forward-angle analyzing power is very large. Inclusion of the MM interaction also gives a much better description of the angular distribution of the medium-energy ($T_{\rm lab} \lesssim 225$ MeV) depolarization and rotation parameters (for a definition of these observables, see Ref. [52]). This is shown in Table I, where we divided the $\chi^2$ contributions for the 10–350-MeV analyses according to the different types of data, i.e., differential cross sections $\sigma(\theta)$, analyzing powers $A_y$, spin-correlation parameters ($A_{xx}, C_{nn}$, etc.), depolarization parameters ($D$), rotation parameters ($R, A, R', A'$), and the remaining data (polarization transfer parameters $D_t$ and higher-rank spin tensors). Here the numbers in the second column include the normalization data. For example, our data base in the 10–350-MeV energy range contains 506 $\sigma(\theta)$ data divided over several groups, of which 21 have a normalization error. So the number in the second column is given as 527.

### B. np analysis

We will next discuss the effects of the MM interaction in our phase-shift analysis of the *np* scattering data. At the moment, we do not have a satisfactory fit to the *np* data in the 0–350-MeV energy range, and so we will here restrict ourselves to the data below $T_{\rm lab} = 30$

MeV. However, the effect of the MM interaction on the description of these low-energy data is already significant (contrary to the effect of the MM interaction on the description of the *pp* data in this energy range, which is of negligible importance). Some of the results of our *np* analysis without the MM interaction have already been published [53,54], and a full account of our *np* phase-shift analysis will be published elsewhere. Here, we will only briefly give some of the details of our parametrization.

In our *np* analysis, the em part of the long-range interaction consists of the MM potential only. In coordinate space the long-range part of this potential is given by

$$V_{\mathrm{MM}}(r) = -\frac{\alpha\kappa_n}{2M_n}\left[\frac{\mu_p}{2M_p}S_{12} + \frac{1}{M}\left(\mathbf{L}\cdot\mathbf{S} + \mathbf{L}\cdot\mathbf{A}\right)\right]\frac{1}{r^3} \ , \tag{43}$$

where we defined $\mathbf{A} = \frac{1}{2}(\boldsymbol{\sigma}_1 - \boldsymbol{\sigma}_2)$, and $M$ is the neutron-proton reduced mass. Next to the spin-orbit ($\mathbf{L}\cdot\mathbf{S}$) part, this potential also contains an antisymmetric spin-orbit ($\mathbf{L}\cdot\mathbf{A}$) part. This antisymmetric spin-orbit part gives rise to the spin-flip amplitude $M_{ST}$ and the spin-singlet spin-triplet mixing angle $\gamma_l$. For the nuclear part of the potential tail, we take the OPE potential, where we explicitly account for differences between the neutral and charged pion masses, and between proton and neutron masses. We also allow for a difference between the neutral and charged pion-nucleon coupling constants. For the neutral pion-nucleon coupling constant we take the result of our 0–350-MeV *pp* phase-shift analysis [49], $f_0^2 = 74.9 \times 10^{-3}$ (i.e., $g_0^2 = 13.5$), whereas for the charged coupling constant we take the value as determined from $\pi N$ scattering [55], $f_c^2 = 78.9 \times 10^{-3}$ (i.e., $g_c^2 = 14.3$). Here $f$ denotes the pseudovector coupling constant and $g$ the pseudoscalar coupling constant.

To parametrize the short-range interaction, we use an energy-dependent $P$-matrix parametrization in the isospin $I = 0$ lower partial waves with $J \leq 2$. In order to arrive at the correct scattering length, the ${}^1S_0$ phase shift is also parametrized with a $P$ matrix. The other $I = 1$ partial-wave phase shifts with $J \leq 2$ are taken from our 0–30-MeV *pp* phase-shift analysis [10], after correcting them for Coulomb and mass difference effects (see also Ref. [54]). All higher partial waves are taken to be pure OPE.

Some of the *np* data are rejected because of our criterion that data should not be off more than three standard deviations. This leaves us with 445 scattering observables and 54 normalization data. The *np* analysis without the MM interaction gives $\chi^2_{\mathrm{min}} = 475.4$. In this analysis, the more recent accurate analyzing power data give relatively high contributions to $\chi^2_{\mathrm{min}}$. These analyzing power data are the data of Sromicki*et al.* [56] at 25.0 MeV, the data of Holslin *et al.* [20] at 10.03 MeV, and the data of Tornow *et al.* [21] at 16.9 MeV (which include corrections to some earlier measurement by the same group [57]). The reason is partly due to the following. The analyzing power $A_y$ can be written in terms of phase shifts according to (see, e.g., Ref. [58])

$$\sigma(\theta)A_y(\theta) = \frac{\sin^2\delta({}^1S_0)}{4k^2}12\Delta_{LS}\sin\theta \ ,$$

where $\sigma(\theta)$ is the differential cross section and $\Delta_{LS}$ is the spin-orbit combination of the triplet $P$ waves given by

$$\Delta_{LS} = \left[-2\delta({}^3P_0) - 3\delta({}^3P_1) + 5\delta({}^3P_2)\right]/12 \ .$$

The angular dependence of $\sigma(\theta)$ in this energy range is only very small, and so the analyzing power is almost completely determined by the spin-orbit interaction. However, the spin-orbit phase shift in this *np* phase-shift analysis is taken from our *pp* phase-shift analysis [10], after correcting it for Coulomb and mass difference effects. This parametrization contains no free adjustable parameters, and so it is possible that this way of parametrizing the spin-orbit phase shift is not good enough for a proper description of the aforementioned *np* $A_y$ measurements. We therefore also tried an effective-range parametrization for the $\Delta_{LS}$ phase shift:

$$k^3 \cot(\Delta_{LS}) = -\frac{1}{a_{LS}} \; , \tag{44}$$

where $a_{LS}$ is to be fitted to the data. We then indeed find a drop in $\chi^2_{\rm min}$, as is shown in the third column of Table II. The drop is mainly due to a better description of the $A_y$ data. This is shown more explicitly in Table II, in that we separately included the $\chi^2$ contributions to $\chi^2_{\rm min}$ of the total cross sections $\sigma_{\rm tot}$, the differential cross sections $\sigma(\theta)$, the analyzing powers $A_y$, and the spin-correlation parameters $A_{yy}$. The numbers in the second column again refer to the number of scattering observables plus normalization data.

When we next include the MM interaction in the analysis, there is an additional drop of 16 in $\chi^2_{\rm min}$, which is almost totally because of a better description of the forward-angle analyzing power data. This is demonstrated in Fig. 2, where we show the 10.03-MeV analyzing power with and without the MM interaction included. The inclusion of the MM interaction gives rise to a forward-angle dip structure which is in agreement with the experimental data of Holslin *et al.* [20] at this energy. The dip structure is rather large and is only partially shown in Fig. 2. At higher energies the effect of the MM interaction is less pronounced, as is demonstrated in Fig. 2 for the 16.9-MeV data of Tornow *et al.* [21].

If we do not include these 27 accurate analyzing power data of Holslin *et al.* [20] and of Tornow *et al.* [21], the effect of the MM interaction is much smaller. In that case the analysis without the MM interaction results in $\chi^2_{\rm min} = 409.7$, whereas the analysis with the MM interaction results in $\chi^2_{\rm min} = 402.6$. On the other hand, we can also include the preliminary accurate analyzing power measurements of Tornow [22] in our original data base (i.e., the data base including the 10.03- and 16.9-MeV $A_y$ data). These data are given at energies between 7.6 and 18.5 MeV. Because of these low energies, the effects of the MM interaction are expected to be large. The difference in $\chi^2_{\rm min}$ due to the MM interaction is now indeed found to be almost 3 times as large. The final data of these measurements have not yet been published as far as we know, and so our results are only qualitative.

A remark on the treatment of the total cross-section data in the *np* analysis including the MM interaction is in order here. The total cross section is given by $\sigma_{\rm tot} = \int d\phi d\cos\theta \sigma(\theta)$, where

$$\sigma(\theta) = \tfrac{1}{2}\left(|a|^2 + |b|^2 + |c|^2 + |d|^2 + |e|^2 + |f|^2\right) \; .$$

Inspection of the MM amplitudes $e$ and $f$ of Eq. (6) shows that the differential cross section at very small angles behaves as

$$\sigma(\theta) \sim \sin^2\theta/(1-\cos\theta)^2 \; ,$$

which means that $\sigma_{\text{tot}}$ is infinite [35]. However, the singular behavior of $\sigma(\theta)$ occurs at angles that are extremely small (less than 0.1°). Experimentalists usually do not measure these extreme forward angles when they determine $\sigma_{\text{tot}}$. So the value for the total cross section as given by the experimentalists should rather be compared with the value calculated while neglecting the contribution of the MM interaction in these extreme forward angles. In that case the total cross section can be excellently approximated using the optical theorem

$$\sigma_{\text{tot}} = \frac{\pi}{k}\text{Im}\left(M_{SS} + M_{11} + M_{00} + M_{-1-1}\right)(\theta = 0) \;, \tag{45}$$

which does not contain the forward-angle singularity when $F_1^n \equiv 0$. In our analysis, $\sigma_{\text{tot}}$ is calculated using expression (45).

We finally mention that for the *np* analysis we can also make the approximation as used by Arndt *et al.* [11,12] for including the MM interaction. In that case, the MM scattering amplitude is included in all partial waves, but the partial-wave nuclear amplitudes are not adjusted for this. We then find $\chi^2_{\text{min}} = 433.4$, which is almost as good as the more complete treatment discussed in this paper.

## VII. CONCLUSION

From the results of the *pp* and *np* analyses discussed in this paper, we can conclude that the MM interaction has to be included in a phase-shift analysis. Most of the approximations for including the MM interaction that have appeared in the literature are no longer adequate. Especially, accurate forward-angle analyzing power data for both *pp* and *np* scattering require a proper treatment of the MM interaction if they are to be described correctly. The MM interaction has to be included in *all* partial waves, and the nuclear amplitude has to be adjusted accordingly. Without this adjustment the nuclear phase shifts that parametrize the nuclear amplitude are not properly separated from the electromagnetic phase shifts. However, such a deficiency can be largely overcome in a phase-shift analysis, since these phase shifts are parametrized anyway. The parameters in that case can partially simulate the effects of the adjustment of the nuclear phase shifts. This explains why the treatment of Arndt *et al.* for including the MM interaction (treatment D as defined in Sec. VI A) gives results which are almost as good as the more complete treatment E. The approximation D has the advantage over our more complete treatment E, in that it can be included very easily in a phase-shift analysis and gives reasonably good results. However, when more accurate *pp* and *np* scattering data (especially analyzing power data) become available, this approximation will no longer be sufficient.

Similarly, the approximated treatment is no longer correct when the phase shifts parametrizing the nuclear amplitude contain no adjustable parameters. Such a situation occurs if one wants to compare some nucleon-nucleon potential model prediction with the experimental data. The nuclear amplitude in that case is constructed using the phase shifts of the potential model and contains no free parameters. So there are no parameters that can simulate the electromagnetic adjustment of the partial-wave nuclear amplitudes as in Eq. (40). These adjustment factors now have to be included explicitly. The approximated treatments of the contribution of the MM interaction lead to incorrect potential model predictions. This was explicitly demonstrated by us [17] for the 50.04-MeV $A_y$ data of Smyrski *et al.* [16], and the effect of the incorrect treatment of the MM interaction on the potential model comparison with these data is dramatically shown in Fig. 2 of that paper (Ref. [17]).


## ACKNOWLEDGMENTS

We would like to thank Dr. T. Rijken and Drs. R. Timmermans for numerous helpful discussions.

# REFERENCES


[1] N.F. Mott, Proc. Roy. Soc. London, Sect. A **124**, 425 (1929).
[2] J. Schwinger, Phys. Rev. **73**, 407 (1948).
[3] G. Breit, Phys. Rev. **99**, 1581 (1955).
[4] M.E. Ebel and M.H. Hull, Jr., Phys. Rev. **99**, 1596 (1955).
[5] G. Breit and H.M. Ruppel, Phys. Rev. **127**, 2123 (1962).
[6] A. Garren, Phys. Rev. **101**, 419 (1956).
[7] J.D. Hutton, W. Haeberli, L.D. Knutson, and P. Signell, Phys. Rev. Lett. **35**, 429 (1975).
[8] L.D. Knutson and D. Chiang, Phys. Rev. C **18**, 1958 (1978).
[9] M.S. Sher, P. Signell, and L. Heller, Ann. Phys. (N.Y.) **58**, 1 (1970).
[10] J.R. Bergervoet, P.C. van Campen, W.A. van der Sanden, and J.J. de Swart, Phys. Rev. C **38**, 15 (1988).
[11] R.A. Arndt, L.D. Roper, R.A. Bryan, R.B. Clark, B.J. VerWest, and P. Signell, Phys. Rev. D **28**, 97 (1983).
[12] R.A. Arndt, J.S. Hyslop III, and L.D. Roper, Phys. Rev. D **35**, 128 (1987).
[13] J. Bystricky, C. Lechanoine-Leluc, and F. Lehar, J. Phys. (Paris) **48**, 199 (1987).
[14] D.V. Bugg, J.A. Edgington, C. Amsler, R.C. Brown, C.J. Oram, K. Shakarchi, N.M. Stewart, G.A. Ludgate, A.S. Clough, D. Axen, S. Jaccard, and J. Vávra, J. Phys. G **4**, 1025 (1978).
[15] R. Dubois, D. Axen, R. Keeler, M. Comyn, G.A. Ludgate, J.R. Richardson, N.M. Stewart, A.S. Clough, D.V. Bugg, and J.A. Edgington, Nucl. Phys. **A377**, 554 (1982).
[16] J. Smyrski, St. Kistryn, J. Lang, J. Liechti, H. Lüscher, Th. Maier, R. Müller, M. Simonius, J. Sromicki, F. Foroughi, and W. Haeberli, Nucl. Phys. **A501**, 319 (1989).
[17] V.G.J. Stoks and J.J. de Swart, Nucl. Phys. **A514**, 309 (1990).
[18] W.S. Hogan and R.G. Seyler, Phys. Rev. C **1**, 17 (1970).
[19] D.V. Bugg, J.A. Edgington, W.R. Gibson, N. Wright, N.M. Stewart, A.S. Clough, D. Axen, G.A. Ludgate, C.J. Oram, L.P. Robertson, J.R. Richardson, and C. Amsler, Phys. Rev. C **21**, 1004 (1980).
[20] D. Holslin, J. McAninch, P.A. Quin, and W. Haeberli, Phys. Rev. Lett. **61**, 1561 (1988).
[21] W. Tornow, C.R. Howell, M.L. Roberts, P.D. Felsher, Z.M. Chen, R.L. Walter, G. Mertens, and I. Šlaus, Phys. Rev. C **37**, 2326 (1988).
[22] W. Tornow, 1989, private communication; published as G.J. Weisel, W. Tornow, C.R. Howell, P.D. Felsher, M. AlOhali, Z.P. Chen, R.L. Walter, J.M. Lambert, P.A. Treado, and I. Slaus, Phys. Rev. C **46**, 1599 (1992).
[23] J. Bystricky, F. Lehar, and P. Winternitz, J. Phys. (Paris) **39**, 1 (1978).
[24] P. La France and P. Winternitz, J. Phys. (Paris) **41**, 1391 (1980).
[25] H.P. Stapp, University of California Radiation Laboratory Report UCRL-3098, August, 1955.
[26] M.J. Moravcsik, J. Pauschenwein, and G.R. Goldstein, J. Phys. (Paris) **50**, 1167 (1989).
[27] C. Lechanoine, F. Lehar, F. Perrot, and P. Winternitz, Nuovo Cimento **56A**, 201 (1980).
[28] P. La France, C. Lechanoine, F. Lehar, F. Perrot, L. Vinet, and P. Winternitz, Nuovo Cimento A **64**, 179 (1981).
[29] R. Hofstadter, F. Bumiller, and M.R. Yearian, Rev. Mod. Phys. **30**, 482 (1958).

[30] R.J. Budnitz, J. Appel, L. Carroll, J. Chen, J.R. Dunning, Jr., M. Goitein, K. Hanson, D. Imrie, C. Mistretta, J.K. Walker, and R. Wilson, Phys. Rev. **173**, 1357 (1968).
[31] P.N. Kirk, M. Breidenbach, J.I. Friedman, G.C. Hartmann, H.W. Kendall, G. Buschhorn, D.H. Coward, H. DeStaebler, R.A. Early, J. Litt, A. Minten, L.W. Mo, W.K.H. Panofsky, R.E. Taylor, B.C. Barish, S.C. Loken, J. Mar, and J. Pine, Phys. Rev. D **8**, 63 (1973).
[32] M.H. MacGregor, M.J. Moravcsik, and H.P. Stapp, Annu. Rev. Nucl. Sci. **10**, 291 (1960).
[33] H.P. Stapp, T.J. Ypsilantis, and N. Metropolis, Phys. Rev. **105**, 302 (1957).
[34] A. Gersten, Nucl. Phys. **A290**, 445 (1977).
[35] A. Gersten, Phys. Rev. C **18**, 2252 (1978).
[36] M.H. Partovi and E.L. Lomon, Phys. Rev. D **2**, 1999 (1970).
[37] J.J. de Swart and M.M. Nagels, Fortschr. Phys. **26**, 215 (1978).
[38] R. Blankenbecler and R. Sugar, Phys. Rev. **142**, 1051 (1966); A.A. Logunov and A.N. Tavkhelidze, Nuovo Cimento **29**, 380 (1963).
[39] G.J.M. Austen, Ph. D. thesis, University of Nijmegen, 1982 (unpublished).
[40] G.J.M. Austen and J.J. de Swart, Phys. Rev. Lett. **50**, 2039 (1983).
[41] E.A. Uehling, Phys. Rev. **48**, 55 (1935).
[42] L. Durand III, Phys. Rev. **108**, 1597 (1957).
[43] L.C. Biedenharn, J.L. McHale, and R.M. Thaler, Phys. Rev. **100**, 376 (1955).
[44] I.S. Gradshteyn and I.M. Ryzhik, *Table of Integrals, Series, and Products*, Academic Press, 1965.
[45] W.A.M. van der Sanden (unpublished).
[46] M.L. Gursky and L. Heller, Phys. Rev. **136**, B1693 (1964).
[47] J.P. Naisse, Nucl. Phys. **A278**, 506 (1977).
[48] J. Bystricky, A. Gersten, A. Junod, and F. Lehar, Nucl. Phys. **A285**, 469 (1977).
[49] J.R. Bergervoet, P.C. van Campen, R.A.M. Klomp, J.-L. de Kok, T.A. Rijken, V.G.J. Stoks, and J.J. de Swart, Phys. Rev. C **41**, 1435 (1990).
[50] M.M. Nagels, T.A. Rijken, and J.J. de Swart, Phys. Rev. D **17**, 768 (1978).
[51] M.D. Barker, P.C. Colby, W. Haeberli, and P. Signell, Phys. Rev. Lett. **48**, 918 (1982); **49**, 1056E (1982).
[52] L. Wolfenstein, Phys. Rev. **96**, 1654 (1954).
[53] V.G.J. Stoks, P.C. van Campen, W. Spit, and J.J. de Swart, Phys. Rev. Lett. **60**, 1932 (1988).
[54] V.G.J. Stoks, P.C. van Campen, T.A. Rijken, and J.J. de Swart, Phys. Rev. Lett. **61**, 1702 (1988).
[55] O. Dumbrajs, R. Koch, H. Pilkuhn, G.C. Oades, H. Behrens, J.J. de Swart, and P. Kroll, Nucl. Phys. **B216**, 277 (1983).
[56] J. Sromicki, D. Holslin, M.D. Barker, P.A. Quin, and W. Haeberli, Phys. Rev. Lett. **57**, 2359 (1986).
[57] W. Tornow, P.W. Lisowski, R.C. Byrd, and R.L. Walter, Phys. Rev. Lett. **39**, 915 (1977); Nucl. Phys. **A340**, 34 (1980).
[58] G.S. Mutchler and J.E. Simmons, Phys. Rev. C **4**, 67 (1971).

## TABLES

TABLE I. $\chi^2_{\rm min}$ values for the different treatments A–F of the MM interaction for the 0–350- and 10–350-MeV analyses. For the latter analysis a division is made giving the sub-$\chi^2$ on the differential cross sections, analyzing powers, spin-correlation parameters, depolarization parameters, rotation parameters, and the remaining data.

| Energy range | $N_{\rm dat}$ | A | B | C | D | E | F |
|---|---|---|---|---|---|---|---|
| 0–350 MeV | 1766 | 1907.3 | 2377.3 | 1872.1 | 1783.9 | 1785.0 | 1765.0 |
| 10–350 MeV | 1431 | 1603.2 | 1540.0 | 1537.2 | 1483.8 | 1474.1 | 1455.6 |
| $\sigma(\theta)$ | 527 | 579.8 | 583.0 | 580.9 | 561.7 | 557.9 | 551.0 |
| $A_y$ | 497 | 591.1 | 560.0 | 564.8 | 535.3 | 535.2 | 531.3 |
| $A_{xx}, C_{nn}, \ldots$ | 65 | 55.8 | 54.7 | 54.4 | 54.3 | 53.1 | 52.6 |
| $D$ | 88 | 133.5 | 114.3 | 110.8 | 108.2 | 104.3 | 102.1 |
| $R, A, R', A'$ | 209 | 217.2 | 201.9 | 200.2 | 198.0 | 197.7 | 192.2 |
| remainder | 45 | 25.8 | 26.1 | 26.1 | 26.2 | 26.0 | 26.4 |

TABLE II. $\chi^2_{\rm min}$ values for the different $np$ phase-shift analyses with $T_{\rm lab} \leq 30$ MeV. The last two columns refer to the analyses where the $\Delta_{LS}$ phase shift is given by an effective-range parametrization. For all analyses a division is made giving the sub-$\chi^2$ on the total cross sections, the differential cross sections, the analyzing powers, and the spin-correlation parameters.

| | | | $LS$ effective range | |
|---|---|---|---|---|
| | $N_{\rm data}$ | No MM | No MM | With MM |
| | 499 | 475.4 | 447.3 | 431.7 |
| $\sigma_{\rm tot}$ | 101 | 96.0 | 97.2 | 97.1 |
| $\sigma(\theta)$ | 169 | 141.7 | 140.5 | 140.3 |
| $A_y$ | 222 | 222.4 | 197.0 | 178.9 |
| $A_{yy}$ | 7 | 15.3 | 12.7 | 15.3 |

FIGURES

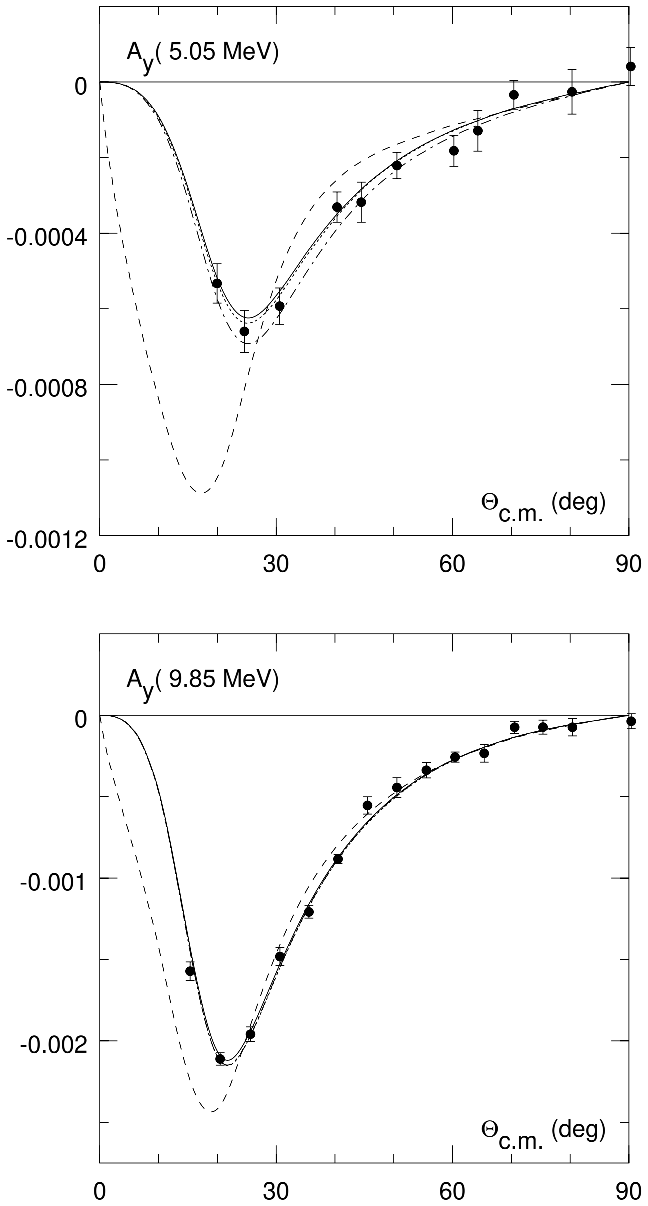


FIG. 1. Effects of the different treatments of the MM interaction for the *pp* analyzing power data at 5.05 and 9.85 MeV of Barker *et al.* [51]. Dotted line: treatment A; dashed line: treatment B; dash-dotted line: treatment D; solid line: treatment E. Details are given in the text.

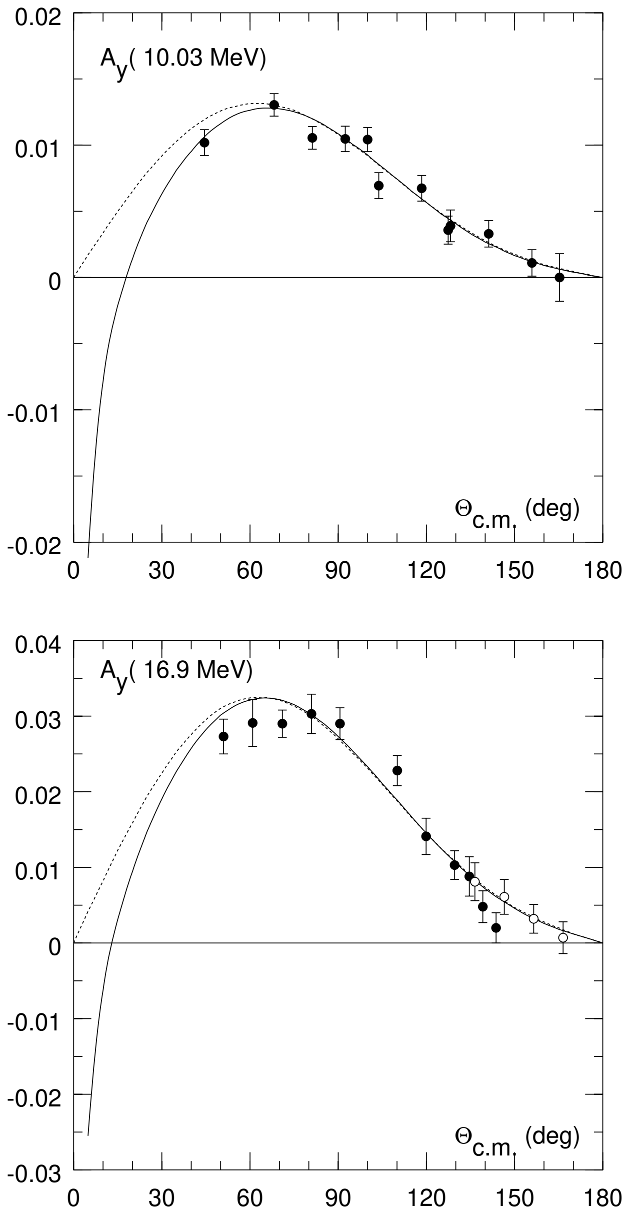


FIG. 2. Effects of the MM interaction for the $np$ analyzing power data at 10.03 MeV of Holslin *et al.* (Ref. [20]) and 16.9 MeV of Tornow *et al.* (Ref. [21]). Dotted line: no MM interaction included; solid line: MM interaction included. The forward-angle dip structure for the analysis including the MM interaction is only partially shown.